

# Bovine Serum Albumin Adsorption onto Colloidal Al<sub>2</sub>O<sub>3</sub> Particles: A New Model Based on Zeta Potential and UV–Vis Measurements

Kurosch Rezwan,\* Lorenz P. Meier, Mandana Rezwan, Janos Vörös, Marcus Textor, and Ludwig J. Gauckler

*Nonmetallic Inorganic Materials, Department of Materials, ETH Zurich, Wolfgang-Pauli-Strasse 10, 8093 Zurich*

*Received June 22, 2004. In Final Form: August 16, 2004*

We investigated the adsorption of bovine serum albumin (BSA) on colloidal Al<sub>2</sub>O<sub>3</sub> particles in an aqueous environment. Changes in the zeta potential of the Al<sub>2</sub>O<sub>3</sub> particles upon the adsorption of BSA were measured using an electro-acoustic technique. The mass of protein adsorbed was determined by using UV–vis spectroscopy. The change of the isoelectric point of the Al<sub>2</sub>O<sub>3</sub> powder–protein suspension was found to be a function of adsorbed protein mass. It was shown that approximately one monolayer of BSA was needed to fully mask the surface and to compromise the charge of Al<sub>2</sub>O<sub>3</sub>. From titration experiments it follows that about 30–36% of the negatively charged groups of the protein form bonds with the protonated and charged Al<sub>2</sub>O<sub>3</sub> surface. On the basis of our observations we introduced a new adsorption model for BSA on Al<sub>2</sub>O<sub>3</sub> particles.

## Introduction

Protein adsorption on surfaces of biomaterials and medical implants is an essential aspect of the cascade of biological reactions taking place at the interface between a synthetic material and the biological environment. Type, amount, and conformation of adsorbed proteins mediate subsequent adhesion, proliferation, and differentiation of cells and are believed to steer foreign body response and inflammatory processes.<sup>1–3</sup>

Interfaces of proteins and metal oxides are not only relevant to the field of biomedical implants but are also crucial for the design of biosensors. Enzymes, for example, are immobilized on hydrophilic materials, where they act as bioselective catalysts for specific cracking of biomolecules.<sup>4–7</sup> A high enzyme activity is desired to achieve a high turnover. We showed in an earlier feasibility study the possibility of using metal oxide particles with a high specific surface area for biosensor applications with a high turnover.<sup>8</sup>

Many different experimental techniques are available for the in situ monitoring of protein adsorption and desorption onto planar metal oxide surfaces such as ellipsometry, optical waveguide light mode spectroscopy, and quartz crystal microbalance.<sup>1,9–12</sup> The drawback of

these methods is the lack of direct information about surface charges, which are known to strongly affect protein adhesion and conformation at interfaces.<sup>13–19</sup> Streaming potential measurements on flat surfaces has been reported in the literature<sup>20</sup> but was rarely used to characterize protein–interface interactions.

By using colloidal oxide particles, we can quantify parameters such as the surface charge, the zeta potential, and the size while at the same time taking advantage of the high surface area for enzyme activity measurements.

Colloidal oxide particles are in most cases polycrystalline, and, thus, no crystal orientation dependent investigations can be carried out. But as far as bioimplants are concerned, the ceramic or metal interfaces always consist of polycrystalline materials as well. Thus, powder particles appropriately represent implant materials with an average over many crystallographic surfaces.

The electrostatic interactions between ceramic particles and proteins are fragmentarily investigated and poorly understood.<sup>21–33</sup> Furthermore, the role of conformational

\* To whom correspondence should be addressed. E-mail: kurosch.rezwan@mat.ethz.ch. Phone: ++41 1 632 6853. Fax: ++41 1 632 1132.

(1) Brunette, D. M.; Tengvall, P.; Textor, M.; Thomson, P. *Titanium in Medicine – Material Science, Surface Science, Engineering, Biological Responses and Medical Applications*; Springer: New York, 2001.

(2) Bucciantini, M.; Fabrizio Chiti, E. G.; Baroni, F.; Formigli, L.; Zurdo, J.; Taddei, N.; Ramponi, G.; Dobson, C. M.; Stefani, M. *Nature* **2002**, *416*, 507.

(3) Bonfield W. T. K. E. *Materials World* **1997**, *5*, 18.  
(4) Shen, B.; Shimmom, S.; Smith, M. M.; Ghosh, P. *J. Pharm. Biomed. Anal.* **2003**, *31*, 83.

(5) Gouda, M. D.; Kumar, M. A.; Thakur, M. S.; Karanth, N. G. *Biosens. Bioelectron.* **2002**, *17*, 503.

(6) Kumar, C. V.; Chaudhari, A. *J. Am. Chem. Soc.* **2000**, *122*, 830.

(7) Lvov, Y. *Anal. Chem.* **2001**, *73*, 4212.

(8) Heule, M.; Rezwan, K.; Cavalli, L.; Gauckler, L. *Adv. Mater.* **2003**, *15*, 1191.

(9) Giacomelli, C. E.; Patricia, M. J. E.; Ortiz, I.; Avena, M. J.; De Pauli, C. P. *J. Colloid Interface Sci.* **1999**, *218*, 404.

(10) Hook, F.; Voros, J.; Rodahl, M.; Kurrat, R.; Boni, P.; Ramsden, J. J.; Textor, M.; Spencer, N. D.; Tengvall, P.; Gold, J.; Kasemo, B. *Colloids Surf., B* **2002**, *24*, 155.

(11) Tanaka, M.; Mochizuki, A.; Motomura, T.; Shimura, K.; Onishi, M.; Okahata, Y. *Colloids Surf., A* **2001**, *193*, 145.

(12) Kurrat, R.; Walivaara, B.; Marti, A.; Textor, M.; Tengvall, P.; Ramsden, J. J.; Spencer, N. D. *Colloids Surf., B* **1998**, *11*, 187.

(13) Roth, C. M. J. E. S.; Lenhoff, A. M. *J. Colloid Interface Sci.* **1998**, *203*, 218.

(14) Servagent-Noinville, S. M. R.; Quiquampoix, H. *J. Colloid Interface Sci.* **2000**, *221*, 273.

(15) Urano, H.; Fukuzaki, S. *J. Biosci. Bioeng.* **2000**, *90*, 105.

(16) Adamczyk, Z. *Adv. Colloid Interface Sci.* **2003**, *100–102*, 267.

(17) Jonsson, B.; Stahlberg, J. *Colloids Surf., B* **1999**, *14*, 67.

(18) Hemar, Y.; Horne, D. S. *J. Colloid Interface Sci.* **1998**, *206*, 138.

(19) Barroug au J. Lemaitre, A.; Rouxhet, P. G. *Colloids Surf.* **1989**, *37*, 339.

(20) Norde W. R. E. *J. Colloid Interface Sci.* **1990**, *139*.

(21) Yuan, Y.; Oberholzer, M. R.; Lenhoff, A. M. *Colloids Surf., A* **2000**, *165*, 125.

(22) Krajewski, A.; Malavolti, R.; Piancastelli, A. *Biomaterials* **1996**, *17*, 7, 53.

(23) Krajewski, A.; Piancastelli, A.; Malavolti, R. *Biomaterials* **1998**, *19*, 637.

(24) Fukuzaki, S.; Urano, H.; Nagata, K. *J. Ferment. Bioeng.* **1996**, *81*, 163.

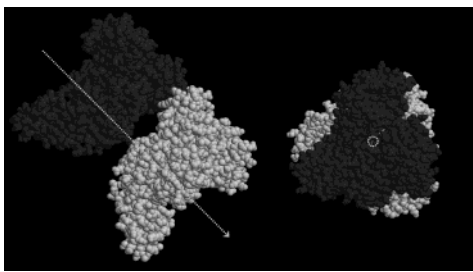


**Figure 1.** Two space filling models from the protein data bank<sup>44</sup> showing a side view (left) and a bottom view of the dimer of the protein. The two chains are distinguished by their shading. The single-headed arrow indicates the viewing direction of the bottom view on the right-hand side. The size of the protein monomer is about  $9 \times 5.5 \times 5.5$  nm.

changes induced by electrostatic interaction during the adsorption process is not clear yet.<sup>34</sup> Preferred orientation modes after adsorption for bovine serum albumin (BSA), such as *side-on* and *end-on*, have been proposed.<sup>15,35,36</sup> The adsorption mechanism is believed to be a multistep process, where the proteins can be found in many different conformational states. This change of conformation upon adsorption is thought to be dependent on the initial protein concentration.<sup>37–41</sup>

In this study we used colloidal  $\text{Al}_2\text{O}_3$  particles which were characterized in terms of the particle size distribution (X-ray disk centrifuge) and purity [differential thermal analysis (DTA), thermogravimetric analysis (TGA), and isoelectric point (IEP)]. The protein that we used was BSA, which is the most abundant protein in bovine blood with a typical concentration of about 50 mg/mL. The molecular weight of BSA is 66 462 g/mol according to literature.<sup>42,43</sup> BSA is a single polypeptide chain consisting of 583 amino acid residues and three domains. High percentages of sequence identities have been noted between BSA and human serum albumin (HSA; 76%) and have been found to be homologous. BSA can also form dimers, especially at high concentrations or in crystallized form.<sup>43</sup> The structure of HSA is illustrated in Figure 1. The structural data for HSA was taken from the online Research Collaboratory for Structural Bioinformatics (RCSB) pro-

**Table 1.** Impurities of the Used  $\text{Al}_2\text{O}_3$  Powder, Supplied by the Company (Taimei)

	impurity (ppm)		impurity (ppm)		impurity (ppm)
Si	3	Na	1	Ca	1
Fe	6	K	1	Mg	1

tein database.<sup>44</sup> Structural data for BSA is not available but is assumed to be very similar because of the high percentage of sequence identities. The IEP of BSA is around 4.7–5, depending on the literature source.<sup>31,45</sup> BSA is negatively charged at pH 7 and undergoes hardly any conformational changes in the pH range from 4 to 8.<sup>43</sup>

In this study we investigated the change of zeta potential as a function of the amount of protein adsorbed on the surface of colloidal alumina particles. We determined the number of charges involved in the adsorption using titration experiments and proposed a new adsorption model based on the results derived from these experiments.

### Experimental Section

**Materials.**  $\text{Al}_2\text{O}_3$  was purchased from Taimei (TM-DAR, lot no. 3973, high purity  $\alpha$ -alumina >99.99%, density 3.98 g/cm<sup>3</sup>) and calcined for 4 h at 400 °C to eliminate any organic residues. Additional data from the supplier can be found in Table 1.

BSA was obtained from Sigma Aldrich in powder form (A 7906, lot no. 12K1608) and was used as received.

Double deionized water with an electrical resistance of >18 M $\Omega$  cm from a Nanopure water system (Barnstead) was used for all experiments.

**Methods. Powder Characterization.** DTA and TGA measurements were conducted to determine the amount of organics in the purchased powder (dust, organic residues) and the temperature at which to calcine the powder to eliminate these impurities. The specific surface area was measured by the BET method using a NOVA 1000 device by Quantachrome. A more-or-less spherical particle morphology was verified by scanning electron microscopy (SEM; LEO 1530). The particle size distribution was measured with an X-ray disk centrifuge (Brookhaven Instruments).

For conductivity measurements, two 40-mL samples of an aqueous 2 vol % suspension of the calcined  $\text{Al}_2\text{O}_3$  were prepared and stirred for 1 and 16 h, respectively. After stirring, each was centrifuged and the conductivity of the supernatant was measured to determine the ionic strength due to salt impurities.

**Protein Characterization: Gel Electrophoresis.** To check the purity of the purchased protein lot, the molecular weight distribution was determined by sodium dodecyl sulfate polyacrylamide gel electrophoresis according to the method of Laemmli.<sup>46</sup>

**Preparation of the  $\text{Al}_2\text{O}_3$  Suspension and Protein Addition.** A 170-mL suspension of 2 vol %  $\text{Al}_2\text{O}_3$  including a specified concentration of protein was prepared in a 250-mL Schott glass bottle for each set of four zeta potential experiments, consisting of a basic and an acidic titration after 1 and 16 h of adsorption at room temperature ( $25 \pm 2$  °C).

For the stock suspension, 13.53 g of  $\text{Al}_2\text{O}_3$  powder were added to 151.6 mL of water and shaken vigorously by hand with a Teflon magnetic stirrer inside the bottle for approximately 1 min. Afterward, the suspension was de-agglomerated for 8 min with an ultrasound horn (UP 200 s, Dr. Hielscher, GmbH) at a pulse rate of 0.8 s and with 100% amplitude, which is at the full power of 200 W. During ultrasonication the suspension was being stirred at 300 rpm and ice-cooled to prevent the suspension from heating.

The required amount of protein (see Table 2) was pre-dissolved in 15 mL of water in a 20-mL pills glass using a test tube shaker. The protein was predissolved to favor homogeneous mixing of the added protein with the stock suspension. In each case, the addition of the 15 mL of water from the dissolved protein solution

(25) Lee, W.-K.; Ko, J.-S.; Kim, H.-M. *J. Colloid Interface Sci.* **2002**, *246*, 70.

(26) Kondo, A.; Oku, S.; Higashitani, K. *J. Colloid Interface Sci.* **1991**, *143*, 214.

(27) Kondo, A.; Higashitani, K. *J. Colloid Interface Sci.* **1992**, *150*, 344.

(28) Kondo, A.; Mihara, J. *J. Colloid Interface Sci.* **1996**, *177*, 214.

(29) Kondo, A.; Oku, S.; Murakami, F.; Higashitani, K. *Colloids Surf., B* **1993**, *1*, 197.

(30) Akihiko Kondo, H. F. *J. Colloid Interface Sci.* **1998**, *198*, 34.

(31) Abramson, H. A. M. L. S.; Gorin, M. H. *Electrophoresis of Proteins*; Hafner Publishing Company, Inc.: New York, 1942.

(32) Giacomelli, C. E. W. N. *J. Colloid Interface Sci.* **2001**, *233*, 234.

(33) Bos, M. A.; Shervani, Z.; Anusiem, A. C. I.; Giesbers, M.; Norde, W.; Kleijn, J. M. *Colloids Surf., B* **1994**, *3*, 91.

(34) Ramsden, J. J. *Q. Rev. Biophys.* **1993**, *27*, 41.

(35) Yoon, J.-Y.; Kim, J.-H.; Kim, W.-S. *Colloids Surf., B* **1998**, *12*, 15.

(36) Su, T. J.; Lu, J. R.; Thomas, R. K.; Cui, Z. F.; Penfold, J. J. *Colloid Interface Sci.* **1998**, *203*, 419.

(37) Calonder, C.; Tie, Y.; Van Tassel, P. R. *Proc. Natl. Acad. Sci. U.S.A.* **2001**, *98*, 10664.

(38) Van Tassel, P. R.; Guemouri, L.; Ramsden, J. J.; Tarjus, G.; Viot, P.; Talbot, J. *J. Colloid Interface Sci.* **1998**, *207*, 317.

(39) Michelle, A.; Brusatori, P. R. V. T. *J. Colloid Interface Sci.* **1999**, *219*, 333.

(40) Tian, M.; Lee, W.-K.; Bothwell, M. K.; McGuire, J. *J. Colloid Interface Sci.* **1998**, *200*, 146.

(41) Beverung, C. J.; Radke, C. J.; Blanch, H. W. *Biophys. Chem.* **1999**, *81*, 59.

(42) Hirayama, K.; Akashi, S.; Furuya, M.; Fukuhara, K. *Biochem. Biophys. Res. Commun.* **1990**, *173*, 639.

(43) Carter, D. C.; Ho, J. X. *Adv. Protein Chem.* **1994**, *45*, 153.

(44) RCSB Protein Data Base. <http://www.pdb.mdc-berlin.de> (accessed May 2004).

(45) Dawson, R. M. C. *Data for Biochemical Research*, 3rd ed.; Clarendon Press: Oxford, 1986.

(46) Laemmli, U. K. *Nature* **1970**, *227*, 680.

**Table 2. Protein Amounts Added Including Corresponding Protein Concentrations and Surface Normalizations**

mass added [g]	protein concentration (relative to water volume) [mg mL <sup>-1</sup> ]	normalized (over powder surface area) [ng cm <sup>-2</sup> ]
0.0181	0.1086	10
0.0905	0.5430	50
0.1809	1.0860	100
0.3618	2.1719	200
0.7237	4.3439	400
1.0855	6.5158	600
1.4474	8.6878	800
1.8092	10.8597	1000

reduced the volume fraction of the stock solution to exactly 2 vol. A protein-free reference sample was prepared by simply adding 15 mL of water to a stock solution. For test samples containing protein, the predissolved protein solution was added to the stock suspension under stirring conditions. The amount of added protein, normalized by the surface of the Al<sub>2</sub>O<sub>3</sub>, is also given in Table 2. The suspensions were left stirring for 1 and 16 h in the Schott bottles with fastened lids.

**Zeta Potential.** After 1 and 16 h of stirring the Al<sub>2</sub>O<sub>3</sub>–protein suspension, 30 mL of the samples were withdrawn for measurements. The samples were titrated, and the corresponding zeta potential and electrical conductivity were measured simultaneously as a function of pH. After each addition of the titrant (base respectively acid) an equilibration time of at least 30 s was allowed. The zeta potential of the suspension was measured using the electroacoustic colloidal vibration current technique<sup>47</sup> in a DT 1200 from Dispersion Technology. This method characterizes the zeta potential by means of a probe that uses ultrasound as a driving force for generating an electroacoustic effect. The probe is a stainless steel cylinder with a diameter of 3 cm and a length of 10 cm with a piezo-electric transducer inside. This transducer converts an electrical tone burst into an acoustic pulse that is then emitted into the suspension. The default frequency is 3 MHz. The ultrasonic pulse generates in the suspension a polarization of the colloid particles and their cloud of counterions which can be detected by two electrodes immersed in the suspension. This polarization signal can be used to compute the zeta potential of the particles using electroacoustic theory.<sup>47</sup>

To elucidate the kinetics, the zeta potential was also monitored as a function of time in a different set of experiments. The pH and ionic strength were kept constant at pH 7.2 with a 10 mM *N*-2-hydroxyethylpiperazine-*N*-2-ethanesulfonic acid buffer. The measurements were conducted in a thermostated glass jacket at a temperature of 25 ± 0.1 °C under stirring conditions (500 rpm). For these time measurements, protein concentrations of 0, 50, and 500 ng/cm<sup>2</sup> were chosen and run for 3000 s (50 min).

**Titration.** A total of 70 mL of an Al<sub>2</sub>O<sub>3</sub> suspension without and with 100 ng/cm<sup>2</sup> BSA was prepared in the same manner as the other suspensions mentioned above. In addition to these titrations, nitrogen-purged H<sub>2</sub>O was titrated to measure the background medium, including the intrinsic acidic and basic constants. Also a BSA solution without particles was prepared at the same 100 ng/cm<sup>2</sup> concentration.

After 1 and after 16 h of equilibration time exactly 35 mL of each sample was titrated with 0.1 N KOH base respectively 0.1 N HNO<sub>3</sub> using the titration unit of the DT 1200. The volume of added base was recorded as a function of pH.

**UV–Vis Absorption.** To determine how much protein was adsorbed on the powder surface, several 30-mL suspensions of 2 vol % Al<sub>2</sub>O<sub>3</sub> were prepared and the corresponding protein amounts were added as described above, including predissolving of the protein. Four samples of 1.5 mL were withdrawn from each suspension after 1 and 16 h of stirring and filled into plastic centrifuge cuvettes. Subsequently, the cuvettes were centrifuged for 10 min at 3800*g* in an Eppendorf 5417R table centrifuge, thermostated at 25 °C. After the first run, the supernatants were removed and transferred to fresh cuvettes. Then a second run was started with the same centrifugation settings. After the second run, the supernatant was removed again and filled into fresh cuvettes. The protein concentrations of these cuvettes with the supernatants were measured by using the Bradford method.<sup>48</sup>

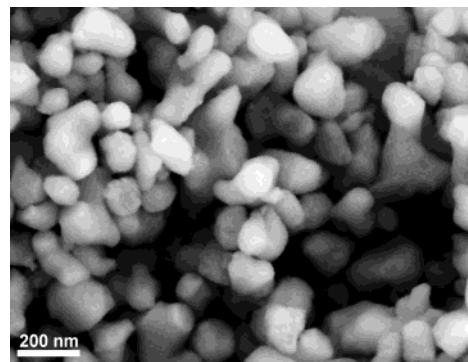


**Figure 2.** SEM micrograph showing the Al<sub>2</sub>O<sub>3</sub> powder which was used for the experiments. The particle morphology is more or less spherical.

For this purpose, prior to the protein concentration measurements, a calibration curve with the used BSA was measured to determine the specific extinction coefficient of the protein. An aqueous dilution series was prepared starting with the start concentration and then diluted to one-half of the original concentration and so forth. The chosen protein detection range was from 0.007 to 0.9 mg/mL. From the protein concentration left in the supernatant and the total amount of protein added in the beginning, the protein amount adsorbed was calculated. The vis absorption values of protein concentration samples were measured at 595 nm, using an UV–vis spectrometer (Lambda 2, Perkin-Elmer).

## Results

**Powder Characterization.** The SEM micrograph in Figure 2 shows the particle morphology of the Al<sub>2</sub>O<sub>3</sub> powder used for the experiments. The particles are more or less spherical. The X-ray disk centrifuge measurement verified the particle size distribution to be monomodal and narrow, with a *d*<sub>50</sub> value of 116 nm, *d*<sub>10</sub> = 82.6 nm, and *d*<sub>90</sub> = 189 nm. The specific surface area of Al<sub>2</sub>O<sub>3</sub> was measured to be 13.37 m<sup>2</sup>/g by BET. The DTA/TGA analysis revealed that all organic impurities were burned out below a temperature of 400 °C. On the basis of this analysis a calcination temperature of 400 °C with a dwell time of 4 h was chosen as a preparation step for the Al<sub>2</sub>O<sub>3</sub> powder for all experiments.

The conductivity of the supernatant of the 2 vol % was 3 μS/cm after 1 h and 10 μS/cm after 16 h. These values correspond to KCl solutions below 0.5 mM.<sup>49</sup>

**Protein Characterization: Gel Electrophoresis.** The molecular weight of the protein lot was found to be 66.2 kDa. Hardly any impurities were detected.

**Zeta Potential.** In Figures 3 and 4 the zeta potential measurements after the addition of different protein amounts are plotted as a function of pH. The IEP of the protein-free Al<sub>2</sub>O<sub>3</sub> was found to be at pH 9.3 after 1 h and at pH 9.0 after 16 h. The IEP decreases with increasing protein amount and levels off at pH 4.9 for 1 h of adsorption time and at pH 5.2 for 16 h of adsorption time. The zeta potential at pH 7 decreases from 70 mV (Al<sub>2</sub>O<sub>3</sub> reference, 1 h) to a minimum of about –15 mV after 1 h of protein adsorption time. The same behavior was observed after 16 h, where the zeta potential decreases from 60 mV to a minimum of about –15 mV.

**Protein Amount Adsorbed: UV–Vis.** In Figure 5 the amount of BSA adsorbed is plotted as a function of the

(47) Dukhin, A. S.; Goetz, P. J. *Ultrasound for Characterizing Colloids. Particle Sizing, Zeta Potential, Rheology*; Elsevier: New York, 2002.

(48) Bradford, M. M. *Anal. Biochem.* **1976**, *15*, 248.

(49) Lide, D. R., Ed. *CRC Handbook of Chemistry and Physics*, 83rd ed.; CRC Press: Boca Raton, 2002.

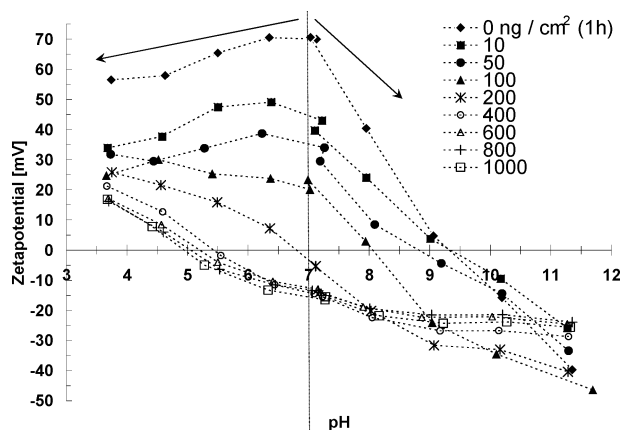


**Figure 3.** Zeta potentials of 2 vol %  $\text{Al}_2\text{O}_3$  suspensions after 1 h of adsorption time for different amounts of added BSA from pH 3.5 to pH 11.5. Each curve consists of two separate sets of five measurements. Titration directions are indicated by the arrows. 0  $\text{ng}/\text{cm}^2$  refers to the  $\text{Al}_2\text{O}_3$  reference suspension without addition of protein.

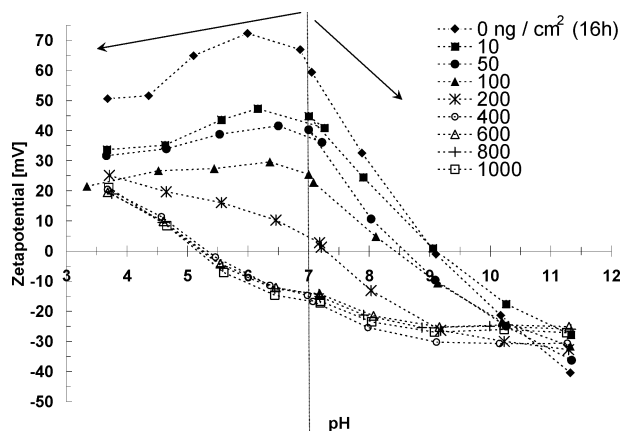


**Figure 4.** Zeta potentials of 2 vol %  $\text{Al}_2\text{O}_3$  suspensions after 16 h of adsorption time for different amounts of BSA added from pH 3.5 to pH 11.5. The 0  $\text{ng}/\text{cm}^2$  refers to the  $\text{Al}_2\text{O}_3$  reference suspension without addition of protein.

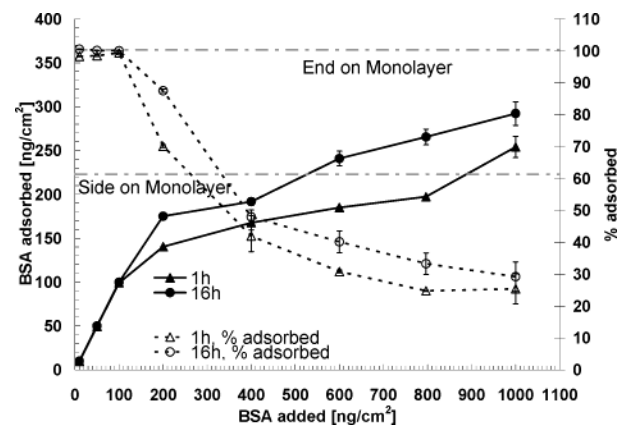


**Figure 5.** BSA adsorption isotherms plotted as a function of BSA added, detected by UV-vis spectroscopy after 1 and 16 h of adsorption time at pH 7. The dotted curves show the relative amount of adsorbed protein. The dotted horizontal lines indicate the calculated amount of BSA needed for *end-on* and *side-on* adsorption modes to cover the surface area with one monolayer.

amount of BSA added for 1 and 16 h of adsorption time. The values are normalized by the surface area. The dotted curves plotted on the secondary axes show the relative amounts of protein adsorbed. Up to a concentration of 100  $\text{ng}/\text{cm}^2$  all of the added BSA is adsorbed after 1 and 16 h.

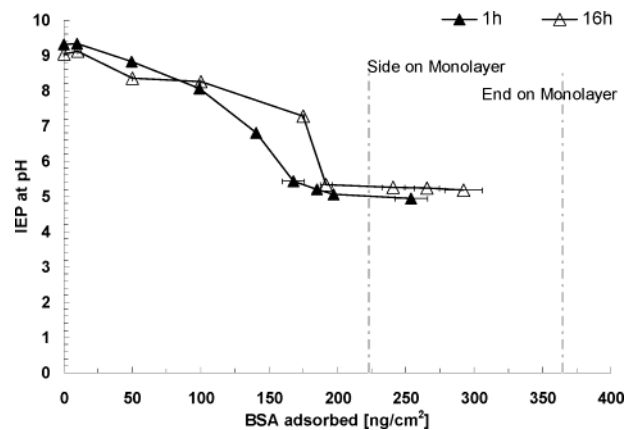


**Figure 6.** IEP of alumina with adsorbed BSA as a function of the effectively adsorbed amount of BSA. The dotted lines indicate the amount which is theoretically needed to form a monolayer for different adsorption modes.

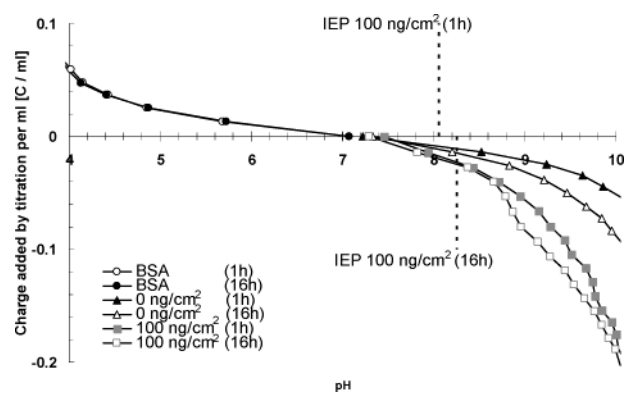


**Figure 7.** Titration curves after 1 and 16 h for BSA, pure  $\text{Al}_2\text{O}_3$ , and 100  $\text{ng}/\text{cm}^2$  BSA adsorbed on  $\text{Al}_2\text{O}_3$  (100% adsorbed). The charge added by titration is dilution- and background-corrected and normalized to 1 mL of volume. The vertical dotted lines indicate the pH values where the corresponding IEPs for the  $\text{Al}_2\text{O}_3$  suspension with an addition of 100  $\text{ng}/\text{cm}^2$  BSA were measured. The other IEPs were not indicated for clarity.

The dotted horizontal lines symbolize the concentration of protein calculated to form a *side-on* and an *end-on* monolayer, assuming a tight packing. Details of these calculations are discussed in Data Analysis and Discussion. In Figure 6 the change of the IEP is plotted as a function of the adsorbed BSA. The curves of this figure were obtained by combining the data of Figures 3–5. Saturation of the IEP (at pH 4.9 and 5.2) was reached at a protein surface coverage of 200  $\text{ng}/\text{cm}^2$ . The vertical dotted lines again symbolize the calculated protein concentration needed to form a monolayer.

**Titration.** In Figure 7 the titration curves after 1 and 16 h for a simple BSA solution, a protein-free  $\text{Al}_2\text{O}_3$  suspension, and an  $\text{Al}_2\text{O}_3$  suspension with added BSA protein at 100  $\text{ng}/\text{cm}^2$  are plotted. This protein concentration of 100  $\text{ng}/\text{cm}^2$  was chosen, after consulting Figure 5, to ensure that 100% of the added BSA was adsorbed on the  $\text{Al}_2\text{O}_3$  surface and that no protein was found anymore in solution at the start of titration. The titrations were started at around pH 7.25.

The amount of titrated charge was calculated from the volume of 0.1 N acid or base that was added and multiplied by Faraday's constant. The added charge was corrected for dilution and background and normalized to a 1-mL suspension volume. The vertical dotted lines in Figure 7 indicate the pH values, where the corresponding IEPs for a BSA addition of 100  $\text{ng}/\text{cm}^2$  were measured after 1 and

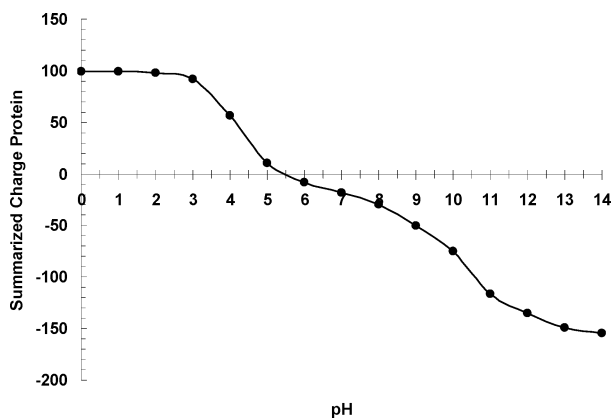


**Figure 8.** Net charge accounting for all charges from BSA. The theoretical IEP was calculated to be at pH 5.56. The IEP of BSA according to data from literature is in the pH range of 4.8–5 in the literature.<sup>31,45</sup>

16 h, derived from Figures 3 and 4. The other IEPs are not shown for clarity.

### Data Analysis and Discussion

**Zeta Potential and Protein Surface Coverage.** The zeta potential measurements conducted at the ionic strength of 10 mM as a function of time at pH 7 reached constant values within 100 s under stirred conditions. Similar time constants were found by others using streaming potential measurements.<sup>20</sup>

The IEP shift for the Al<sub>2</sub>O<sub>3</sub> particles as a function of the added protein reaches saturation at pH 4.9 after 1 h and at pH 5.2 after 16 h of adsorption time (Figures 3 and 4). All adsorption equilibration procedures were conducted at ionic strengths of 1 mM at most as measured by electrical conductivity. The pH values for IEP saturation agree with the IEPs of BSA found in the literature which are between pH 4.7 and pH 5.<sup>31,45</sup> The alumina particles get masked by the protein, and the surface chemistry continuously changes with increasing protein surface coverage from that characteristic of a pure Al<sub>2</sub>O<sub>3</sub> surface to that of the protein. This behavior has also been observed for a small molecule such as citric acid, in which the IEP of Al<sub>2</sub>O<sub>3</sub> shifted continuously from pH 9 to the pK value of citric acid at pH 3 upon specific adsorption of the citric acid.<sup>50</sup>

The IEP of BSA can be calculated by considering the pK values of the side chains of all chargeable amino acids<sup>51</sup> and calculating their dissociation ratios as a function of pH using the buffer equation. The net charge of each amino acid can be obtained by multiplying the dissociation ratios by the number of the corresponding amino acids of the protein (which were obtained from the BSA sequence).<sup>42,43</sup> Summing up the net charge for each amino acid delivers the overall charge of the complete protein as a function of pH, as plotted in Figure 8. A simplification was made in this straightforward calculation by presuming that all amino acids are equally accessible by water, which is not true for the real case. A theoretical pI at pH 5.56 was calculated, which agrees reasonably with the measured IEP at pH 4.9 (1 h) and pH 5.2 (16 h) as well as data from literature ranging from 4.7 to 5.<sup>31,45</sup> For a better understanding, the spatial charge distribution of the protein is visualized in Figure 9 for pH 7. The charged amino acids are uniformly distributed over the whole molecule. The

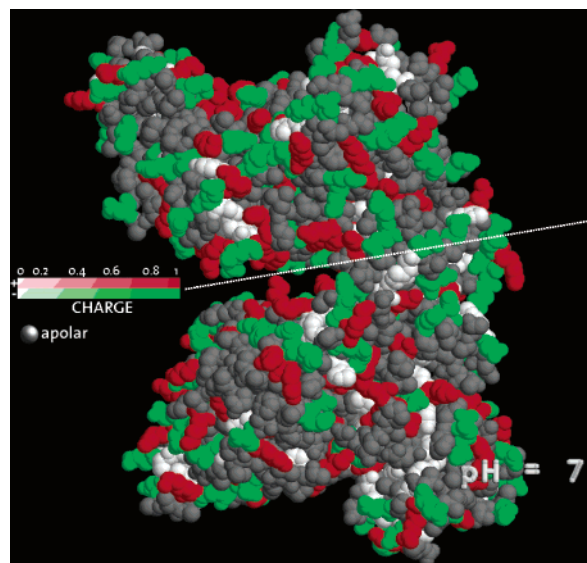


**Figure 9.** Visualization of the calculated charge distribution for a HSA dimer at pH 7. The white spheres are amino acids, which are neutral at pH 7. The gray spheres are apolar or hydrophobic amino groups, which are not charged at any pH. The dotted line indicates where the dimer is assembled.

three-dimensional structure data file taken for the calculations was the structure of HSA, which is almost identical with that of BSA.<sup>43</sup>

By consulting Figure 5, we find that adding 100 ng/cm<sup>2</sup> BSA results in a complete adsorption for 1 and 16 h of adsorption time. Starting with 200 ng/cm<sup>2</sup>, the amount of adsorbed protein differs significantly for 1 and 16 h of adsorption time. The dotted horizontal lines symbolize the calculated amount of protein needed for the two adsorption modes. The BSA monomer structure is heart shaped (Figure 1); hence, two different adsorption areas were calculated for the same protein. One protein area was calculated for the “side-on” mode (9 × 5.5 nm<sup>2</sup>) and one area was calculated for the “end-on” mode (5.5 × 5.5 nm<sup>2</sup>). Both areas were calculated from the three-dimensional structure file of HSA obtained from X-ray diffraction in the protein database.<sup>44</sup> Two different adsorption modes were also suggested by others.<sup>35,52</sup> On the basis of this assumption and taking into account the molecular weight of 66 430.3 g/mol,<sup>43</sup> the amount of BSA needed to cover 1 cm<sup>2</sup> in the side-on mode was calculated to be 223 and 365 ng for the end-on adsorption mode. These two calculated maximum surface coverages are indicated by the straight, dotted lines in Figures 5 and 6. From Figure 5 it can be seen that for protein additions of up to 400 ng/cm<sup>2</sup> the amount of proteins adsorbed on the surface stays below the calculated monolayer concentration that theoretically would be required to form a monolayer in side-on mode. This was found to be true after 1 and 16 h of adsorption time. The protein amount adsorbed after 1 h of adsorption time stays below the side-on monolayer line up to a protein addition of 800 ng/cm<sup>2</sup>. For a protein addition of 1000 ng/cm<sup>2</sup> we find the protein amount adsorbed to be beyond the monolayer limit for side-on adsorption. For the 16-h adsorption curve, the exceeding amount is already found to be at 600 ng/cm<sup>2</sup>.

From Figure 6 it can be seen that at pH 5 the IEP was saturated and no further shift of the IEP was obtained by more protein adsorption. The adsorbed amount of protein where IEP saturation is found is for both 1 and 16 h of

(50) Hidber Pirmin, C.; Graule Thomas, J.; Gauckler Ludwig, J. *J. Am. Ceram. Soc.* **1996**, *79*, 1857.

(51) Stryer, L. *Biochemistry*, 4th ed.; Freeman & Co.: New York, 1997.

(52) Lassen, B.; Malmsten, M. *J. Colloid Interface Sci.* **1996**, *180*, 339.

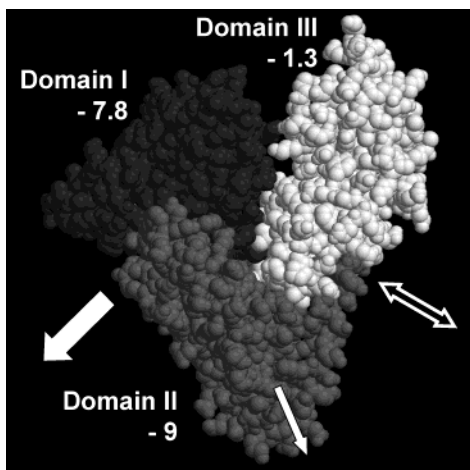


**Figure 10.** The three domains of BSA including the calculated net charges present at pH 7. The double-headed arrow indicates where a second BSA molecule docks for dimer formation. The broad single-headed arrow symbolizes the hypothesized *side-on* adsorption mode with an adsorption area of  $9 \times 5.5 \text{ nm}^2$ . The thin single-headed arrow indicates the *end-on* adsorption mode with an adsorption area of  $5.5 \times 5.5 \text{ nm}^2$ .

adsorption time between 175 and 200  $\text{ng}/\text{cm}^2$ . This protein amount lies reasonably close to the calculated amount for a *side-on* monolayer (223  $\text{ng}/\text{cm}^2$ ). From this observation it can be concluded that roughly one *side-on* monolayer of BSA is necessary to completely change the surface charge of  $\text{Al}_2\text{O}_3$  to the surface charge of BSA.

Two questions arise from these observations: (1) which adsorption mode is dominating and (2) why does BSA still adsorb to the  $\text{Al}_2\text{O}_3$  particles after masking surface charge completely?

Consulting Figure 9 no obvious reasons can be given to answer the question why BSA should adsorb in a preferred mode at pH 7 because the spatial charges seem to be uniformly distributed. But summing up the net charges for each of the three domains reveals an asymmetric charge distribution for the BSA monomer as illustrated by Figure 10 (note: The protein structure data file of HSA was used for the illustration but the domain charge amounts were calculated by using the BSA sequence from Carter and Ho).<sup>43</sup> It can be seen that domains I and II result together in a net charge of  $-16.8$  whereas domain III holds a net charge of only  $-1.3$  at pH 7. A similar asymmetric charge distribution was also reported by others for HSA.<sup>53</sup> This imbalanced charge distribution strongly suggests a *side-on* adsorption on the positively charged  $\text{Al}_2\text{O}_3$  surface as indicated by the broad single-headed arrow in Figure 10 and not an *end-on* adsorption in the direction of the thin single-headed arrow. After formation of the *side-on* monolayer at a surface coverage of around 200  $\text{ng}/\text{cm}^2$ , the *side-on* adsorption would theoretically need to switch to the *end-on* adsorption mode (Figure 5) because of lack of space. But *end-on* mode adsorption is not favored because of the asymmetric charge distribution of the protein (Figure 6). Therefore, we can conclude that, with increasing protein concentration, BSA starts forming dimers at the surface as it “naturally” would do at high concentrations or during crystallization. This conclusion is supported by the fact that after *side-on* adsorption of BSA into the direction of the broad single-headed arrow (Figure 10) the dimer docking sites for a second BSA would still be accessible to form a dimer. We think that at a protein concentration adsorbed on the surface larger than

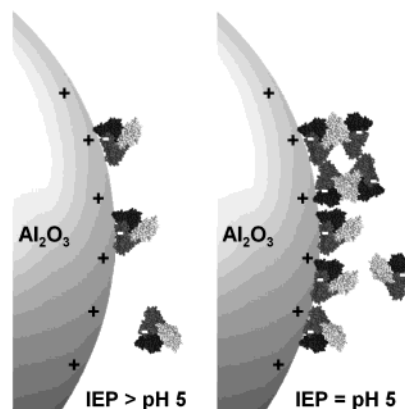


**Figure 11.** Proposed adsorption model for BSA on  $\text{Al}_2\text{O}_3$  particles at pH 7. The protein–particle size ratios are to scale. In the first adsorption phase (left) the *side-on* monolayer is formed. The more protein molecules adsorb, the closer the IEP of alumina (initially at pH 9) moves toward pH 5 (IEP of BSA). After the first adsorption layer, the surface charge of the  $\text{Al}_2\text{O}_3$  particle is masked; that is, the IEP cannot be shifted any further with further addition of BSA (see also Figure 6). In the second adsorption phase (right) the additional BSA molecules form dimers with proteins that are already adsorbed.

200  $\text{ng}/\text{cm}^2$  (as shown in Figure 6, where the IEP of  $\text{Al}_2\text{O}_3$  is masked by the IEP of BSA) further protein adsorption occurs only through protein/protein interactions and no BSA/ $\text{Al}_2\text{O}_3$  surface interactions occur anymore. Protein/protein interactions are manifold and can consist of hydrogen bridges, disulfide bonds, and hydrophobic effects.<sup>54</sup>

The suggested two-step adsorption model at pH 7 is illustrated by Figure 11. During the first adsorption phase (left) the *side-on* monolayer is being formed. At the ionic strengths below 1 mM at which the adsorption equilibration was carried out, the Debye length is about 10 nm. Thus, the initial BSA molecules can orientate during the adsorption process. The more protein molecules adsorb, the more the IEP moves from the IEP of the powder (pH 9) toward the IEP of the protein (pH 5). After the first layer of BSA adsorption, the surface charge of the alumina is completely masked and the IEP cannot be shifted any further than the IEP of the protein (see Figure 6). In the second adsorption phase (right) the subsequently adsorbing BSA molecules form dimers with protein molecules that are already adsorbed. This dimer formation is based on protein/protein interaction and cannot be due to electrostatic interaction with the  $\text{Al}_2\text{O}_3$  particle surface. According to this model, a complete dimer layer would be reached if about 450  $\text{ng}/\text{cm}^2$  (corresponding to two *side-on* layers) adsorbed on the particle surface.

Because during the adsorption process also relaxation of the BSA molecules occurs besides their orientation, the protein layers can also exhibit stacking faults. This becomes more and more important at higher protein concentrations.

**Titration.** The titration curves after 1 and 16 h for dissolved BSA in Figure 7 show no significant differences. This indicates a high reproducibility of the conducted titration experiments. Calculation of the charge needed to reach pH 4.8, which is known to be the IEP of the protein,<sup>31</sup> yields  $-16.50 \text{ e}^-$  after 1 h and  $-16.53 \text{ e}^-$  after 16 h of dissolving time. These results agree very well with the calculated number of charged units presented at pH 7 which was found to be  $-18.01 \text{ e}^-$  (see Figure 8). It is

(53) Peters, T., Jr. *Adv. Protein Chem.* **1985**, *37*, 161.

(54) Thornton, S. J. J. M. *Proc. National Acad. Sci. U.S.A.* **1996**, *93*, 13.

**Table 3. Charge Measured Per Milliliter of Sample from Titration Data**

	charge after 1 h/mL [C/mL]	charge after 16 h/mL [C/mL]
BSA only ( $C_B$ )	-0.0260	-0.0260
0 ng/cm <sup>2</sup> ( $C_0$ )	0.0267	0.0328
100 ng/cm <sup>2</sup> ( $C_{100}$ )	0.0172	0.0248
$C_{100} - C_0$	-0.0094	-0.0079

known from literature<sup>43</sup> that BSA does not undergo any significant conformational changes in the pH range from 4 to 8. Thus, it can be assumed that the number of titratable groups did not change during titration.

From the titration data in Figure 7 for Al<sub>2</sub>O<sub>3</sub> with and without a protein addition of 100 ng/cm<sup>2</sup> BSA, the charges needed to reach the corresponding IEPs (at pH 8.1 respectively 8.3) were also derived. Table 3 shows the results found after 1 and 16 h.

For the following discussion we assumed that the titrated charges are additive because we take only a small titration range around pH 7 into account, which is linear for the calculations, and that charge regulation is negligible. We also assumed that very low amounts of BSA desorb from the alumina surface during the relatively fast titration for these pH ranges and small protein concentrations as found by others for BSA and alumina.<sup>15</sup>

From Table 3 it can be seen that BSA is approximately as highly charged ( $C_B$ ) as Al<sub>2</sub>O<sub>3</sub> but with an opposite sign. However, looking at the charge obtained for Al<sub>2</sub>O<sub>3</sub> with a protein addition of 100 ng/cm<sup>2</sup> BSA ( $C_{100}$ ), we find only a small amount of charge being compromised ( $C_{100} - C_0$ ). This fact suggests that not all positively charged groups of the Al<sub>2</sub>O<sub>3</sub> particle are neutralized after adsorption. We can conclude that not all negatively charged groups of BSA form bonds with positively charged Al<sub>2</sub>O<sub>3</sub> groups and, thus, many Al<sub>2</sub>O<sub>3</sub> groups can be titrated. This explanation is reasonable, considering the fact that the protein has a three-dimensional extension and that it cannot be treated

as a point of charge. Hence, some of the groups are pointing away from the particle surface and some are hampered by steric hindrance from approaching the particle surface.

Knowing how much charge was compromised because of adsorption ( $C_{100} - C_0$ ) and knowing how much charge one BSA molecule carries as calculated earlier, we can derive the percentage of negatively charged groups of the protein forming bonds with the Al<sub>2</sub>O<sub>3</sub> particle. After 1 h, we find 36% of the negatively charged groups of one BSA molecule being neutralized as a result of adsorption and 30% after 16 h.

### Conclusions

In this study we investigated the adsorption of BSA onto colloidal Al<sub>2</sub>O<sub>3</sub> particles.

BSA adsorption on alumina surfaces is a fast process (<100 s) under well-stirred conditions. As a result of the proteins adsorbed on alumina, a shift of the IEP of the Al<sub>2</sub>O<sub>3</sub>/protein suspension was found. This shift is a function of the adsorbed protein mass and reached saturation at pH 5 corresponding to the pI of the protein. IEP saturation was obtained after a monolayer of BSA adsorbed on Al<sub>2</sub>O<sub>3</sub>. Additional proteins form dimers with those from the first monolayer. A two-step adsorption model is proposed for this further protein adsorption based on the observation that, even after the positive surface charge of the Al<sub>2</sub>O<sub>3</sub> particles was fully compromised by the BSA molecules, further protein adsorption can occur.

In titration experiments we found that only 30–36% of the total negative charge of the protein formed bonds with the positively charged Al–hydroxyl surface groups, which was attributed to the three-dimensional form of the protein.

**Acknowledgment.** We thank Dr. André Studart and Dr. Ayesha Ahmad for fruitful discussions and ETH Zurich for financial support.

LA048459K